Identification and validation of a necroptosis-related gene prognostic signature for colon adenocarcinoma

Jingyao Zhang[1#]^, Ziyue Liu[2#]^, Wenhao Chen[1]^, Hengchen Liu[3]^

[1]Department of 'A', Children's Hospital, Zhejiang University School of Medicine, National Clinical Research Center for Child Health, Pediatric Cancer Research Center, Hangzhou, China; [2]Department of Clinical Medicine, The Fifth Affiliated Hospital of Harbin Medical University, Harbin, China; [3]Department of Colorectal Surgery and Oncology, Key Laboratory of Cancer Prevention and Intervention, Ministry of Education, Zhejiang Provincial Clinical Research Center for Cancer, The Second Affiliated Hospital, Zhejiang University School of Medicine, Hangzhou, China

Contributions: (I) Conception and design: J Zhang, Z Liu; (II) Administrative support: W Chen, H Liu; (III) Provision of study materials or patients: H Liu; (IV) Collection and assembly of data: J Zhang; (V) Data analysis and interpretation: J Zhang, H Liu; (VI) Manuscript writing: All authors; (VII) Final approval of manuscript: All authors.

[#]These authors contributed equally to this work.

Correspondence to: Hengchen Liu, MD. Department of Colorectal Surgery and Oncology, Key Laboratory of Cancer Prevention and Intervention, Ministry of Education, Zhejiang Provincial Clinical Research Center for Cancer, The Second Affiliated Hospital, Zhejiang University School of Medicine, 88 Jiefang Road, Hangzhou 310009, China. Email: 2322043@zju.edu.cn; Wenhao Chen, MD. Department of 'A', Children's Hospital, Zhejiang University School of Medicine, National Clinical Research Center for Child Health, Pediatric Cancer Research Center, 3333 Binsheng Road, Hangzhou 310052, China. Email: whchenortho@zju.edu.cn.

Background: Necroptosis is a novel programmed cell death pathway proposed in 2005, which is mainly activated by the tumor necrosis factor (TNF) family and mediates cellular disassembly via receptor interacting serine/threonine kinase 1 (RIPK1), receptor interacting serine/threonine kinase 3 (*RIPK3*) and mixed lineage kinase domain like pseudokinase (*MLKL*). We tried to analyze the relationship of necroptosis-related genes (NRGs) expression with colon adenocarcinoma (COAD) and propose potential therapeutic targets through immunological analysis.

Methods: First, we evaluated the expression of NRGs in COAD patients and constructed a prognostic signature. The prognostic signature was validated using The Cancer Genome Atlas (TCGA)-COAD and GSE39582 datasets, respectively. And the Kaplan-Meier analysis, receiver operating characteristic (ROC) curves, and principal component analysis were used to evaluate the signature. Then we analyzed the enrichment of NRGs in the signature using Gene Ontology (GO) and Kyoto Encyclopedia of Genes and Genomes (KEGG) analyses. Finally, we analyzed the immunological characteristics of the COAD patients by single sample gene set enrichment analysis (ssGSEA) and predicted the possible immune checkpoints.

Results: We constructed a prognostic signature with 8 NRGs (*RIPK3*, *MLKL*, *TRAF2*, *CXCL1*, *RBCK1*, *CDKN2A*, *JMJD7-PLA2G4B* and *CAMK2B*). The Kaplan-Meier analysis, ROC curves, and principal component analysis demonstrated good predictivity of the signature. In addition, we constructed a nomogram with good individualized predictive ability (C-index =0.772). The immunological analysis revealed that the prognosis of COAD was associated with autoimmune function, and we proposed 10 potential therapeutic targets.

Conclusions: Overall, we constructed an NRGs prognostic signature and suggested potential therapeutic targets for the COAD treatment.

Keywords: Colon adenocarcinoma (COAD); The Cancer Genome Atlas (TCGA); Gene Expression Omnibus (GEO); necroptosis; prognosis

---

^ ORCID: Jingyao Zhang, 0000-0001-9790-0803; Ziyue Liu, 0000-0003-1887-7671; Wenhao Chen, 0000-0001-8988-7362; Hengchen Liu, 0000-0001-7263-6735.

Introduction

Colon adenocarcinoma (COAD) is a common digestive tract cancer representing 6% of all cancer cases, with approximately 1 million cases each year (1,2). Due to its insidious onset, the optimal treatment timing is often missed, resulting in high mortality (3). In addition, epidemiological investigations have found that COAD incidence gradually becomes younger (4-6). The incidence of COAD seems to be related to genetics, diet, and inflammation, but the specific mechanism is not well explored (7,8). Although progress has been made in the clinical treatment of COAD with the development of therapies in recent years, the 5-year recurrence rate remains high (9). Therefore, finding newer cancer biomarkers and potential therapeutic targets of COAD are warranted.

Necroptosis is a novel programmed cell death pathway proposed in 2005 (10). Unlike the traditional form of apoptosis, necroptosis is mainly activated by the tumor necrosis factor (TNF) family and mediates cellular disassembly via receptor interacting serine/threonine kinase 1 (*RIPK1*), receptor interacting serine/threonine kinase 3 (*RIPK3*) and mixed lineage kinase domain like pseudokinase (*MLKL*) (11). Necroptosis influences the progression of

many diseases, including myocardial, cerebral ischemia, and acute kidney injury (12-14). Since necroptosis does not affect the programmed cell death when apoptosis gets inhibited, it has attracted extensive attention. However, necroptosis has dual attributes of promoting the development and progression of tumors. Shikonin, a natural compound derived from the dried root of *Lithospermum erythrorhizon*, has shown promising anti-tumor activity. It effectively inhibited the progression and metastasis of various tumors by inducing the necroptosis pathways (15-17). In addition, some chemotherapeutics inhibited tumor growth by activating the necroptosis pathways (18). However, Seifert *et al.* showed that necroptosis promoted the occurrence of pancreatic cancer (19). Liu *et al.* found that the application of necroptosis inhibitor (necrosulfonamide) significantly inhibited the proliferation of breast cancer (20). Thus, the regulation of necroptosis-related genes (NRGs) has the potential to be the key to cancer therapy.

Additionally, necroptosis is involved in the microenvironmental immune responses as immunogenic cell death. Necroptotic tumor cells activate the immune system and promote the activation of dendritic cells (DCs). This process is controlled by the nuclear factor kappa-B (NF-κB) pathway and damage-associated molecular patterns (DAMPs) (21,22). Therefore, necroptosis combined with immunotherapy is a novel therapeutic method in cancer. Several studies have confirmed that NRGs influence the prognosis of liver, breast and colon cancer (23-25). In this study, we focused on the NRGs as an independent prognostic indicator to explore their relationship with COAD prognosis and constructed a prognostic signature containing 8 NRGs. In addition, we attempted to find differences in immunological characteristics and proposed a potential immunotherapeutic target based on the obtained signature. We present this article in accordance with the TRIPOD reporting checklist (available at https://tcr.amegroups.com/article/view/10.21037/tcr-23-494/rc).

Highlight box

Key findings
- In this study, a novel colon adenocarcinoma (COAD) prognosis prediction signature containing 8 necroptosis-related genes (*RIPK3*, *MLKL*, *TRAF2*, *CXCL1*, *RBCK1*, *CDKN2A*, *JMJD7-PLA2G4B* and *CAMK2B*) was constructed.

What is known and what is new?
- Necroptosis is a novel form of cell death, which is closely associated with tumor development.
- The prognostic signature constructed by necroptosis-related genes showed a good predictability in COAD. Furthermore, the necroptosis-related genes were closely related to tumor immunity and 10 potential immune checkpoints for COAD were proposed.

What is the implication, and what should change now?
- The prognostic signature could be used as a useful tool for clinicians to judge the prognosis of patients and develop new therapeutic targets for COAD.

Methods

Data collection and processing

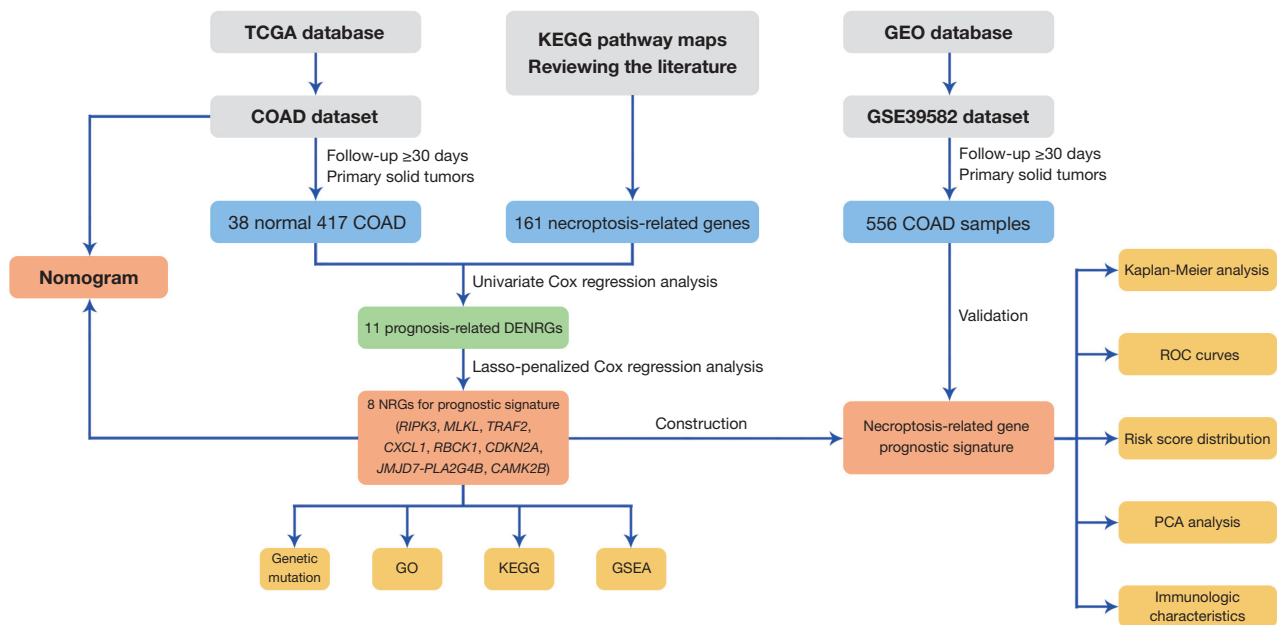The flow chart for this study is shown in *Figure 1*. The

Figure 1 The flow chart of the research process. The flow chart depicts the inclusion criteria for TCGA-COAD and GSE39582 datasets and the process of NRG prognostic signature identification and validation. In addition, the clinical significance was explored based on the signature. TCGA, The Cancer Genome Atlas; KEGG, Kyoto Encyclopedia of Genes and Genomes; GEO, Gene Expression Omnibus; COAD, colon adenocarcinoma; DENRGs, differentially expressed NRGs; NRGs, necroptosis-related genes; ROC, receiver operating characteristic; PCA, principal component analysis; GO, Gene Ontology; GSEA, Gene Set Enrichment Analysis.

sequencing and clinical data of COAD patients were downloaded from The Cancer Genome Atlas (TCGA) database (https://portal.gdc.cancer.gov/) and Gene Expression Omnibus (GEO) database (https://www.ncbi. nlm.nih.gov/geo/). To improve the accuracy of this study, we excluded samples having incomplete clinical information (age, gender, tumor stage, survival status) and selected sequencing data from primary solid tumors. To increase the reliability of the results, we excluded ineffective cases (follow-up days <30). Finally, we selected the relevant data of 38 normal and 417 COAD samples from the TCGA database (*Table 1*). Raw count values of RNA-sequencing (RNA-seq) data were used for screening differentially expressed genes, and fragments per kilo base of transcript per million mapped fragments (FPKM) values [converted to transcripts per million (TPM) values] were used for other studies. In addition, we selected 556 COAD samples in the GSE39582 dataset (*Table 2*). The standard PRISMA flow diagram of the screened samples is shown in Figure S1. The RNA-seq values in GSE39582 were normalized by the RMA algorithm. This study adhered to the publication standards of TCGA and GEO databases. The study was

conducted in accordance with the Declaration of Helsinki (as revised in 2013). No ethics committee approval was required.

Identification of differentially expressed NRGs (DENRGs)

We obtained 161 NRGs by reviewing the literature and the necroptosis-related Kyoto Encyclopedia of Genes and Genomes (KEGG) pathway maps (table available at https:// cdn.amegroups.cn/static/public/tcr-23-494-1.pdf). Next, the DENRGs between normal and COAD samples were downloaded from TCGA as screened by R software [false discovery rate (FDR) <0.05]. The hazard ratios (HRs) were used to evaluate the property of the DENRGs (protective or risk).

Construction and validation of the NRG signature

The prognosis-related DENRGs were identified by univariate Cox regression analysis, and a protein-protein interaction (PPI) network was constructed by STRING. Next, a NRG signature was constructed by Lasso-penalized

Transl Cancer Res 2023;12(9):2239-2255 | https://dx.doi.org/10.21037/tcr-23-494

Table 1 Corresponding clinical features of 417 patients with colon adenocarcinoma in TCGA-COAD

Items	Patients (n=417), n (%)
Age (years)	
<65	161 (38.6)
≥65	256 (61.4)
Gender	
Male	224 (53.7)
Female	193 (46.3)
Tumor stage	
Stage I	75 (18.0)
Stage II	164 (39.3)
Stage III	121 (29.0)
Stage IV	57 (13.7)
Survival status	
Alive	329 (78.9)
Dead	88 (21.1)

TCGA, The Cancer Genome Atlas; COAD, colon adenocarcinoma; N, numbers.

Table 2 Corresponding clinical features of 556 patients with colon adenocarcinoma in GSE39582

Items	Patients (n=556), n (%)
Age (years)	
<65	212 (38.1)
≥65	344 (61.9)
Gender	
Male	307 (55.2)
Female	249 (44.8)
Tumor stage	
Stage I	36 (6.5)
Stage II	258 (46.4)
Stage III	203 (36.5)
Stage IV	59 (10.6)
Survival status	
Alive	369 (66.4)
Dead	187 (33.6)

N, numbers.

Cox regression analysis:

$$\text{Risk Score} = \sum_{i=1}^{n} \left(\text{Exp}_i \times \text{Coef}_i \right) \quad\quad [1]$$

Then TCGA-COAD and GSE39582 datasets were selected to evaluate the reliability of this signature. Next, patients were divided into low- and high-risk groups based on the median value of their risk score, and the distribution of each group was visualized by principal component analysis (PCA). Finally, Kaplan-Meier analysis and receiver operating characteristic (ROC) curves were used to evaluate the predictability of the signature.

Clinical prognostic analysis

We explored the clinical relevance of signature by rank-sum test. Univariate and multivariate Cox regression analyses were used to assess the independent predictive ability of the signature. In addition, we constructed a nomogram to improve individualized prediction ability. The immunohistochemistry images were obtained from the human protein atlas (HPA) database (https://www.proteinatlas.org/).

Genetic mutation, Gene Ontology (GO), KEGG, and gene set enrichment analysis (GSEA)

The data of simple nucleotide variation (SNV) and copy number variation (CNV) of COAD patients were downloaded from the TCGA database. KOBAS-i was used to analyze the GO and KEGG of the genes in the signature. The analysis results were visualized by R software. GSEA was used to find differentially enriched pathways in low- and high-groups [P<0.05, FDR <0.25, |normalized enrichment score (NES)| >1].

Immunological analysis

Immunological characters (immune cells and immunological functions) were assessed between two groups using the single sample GSEA (ssGSEA) algorithm (26). Further, we predicted the potential immune-checkpoints.

Statistical analysis

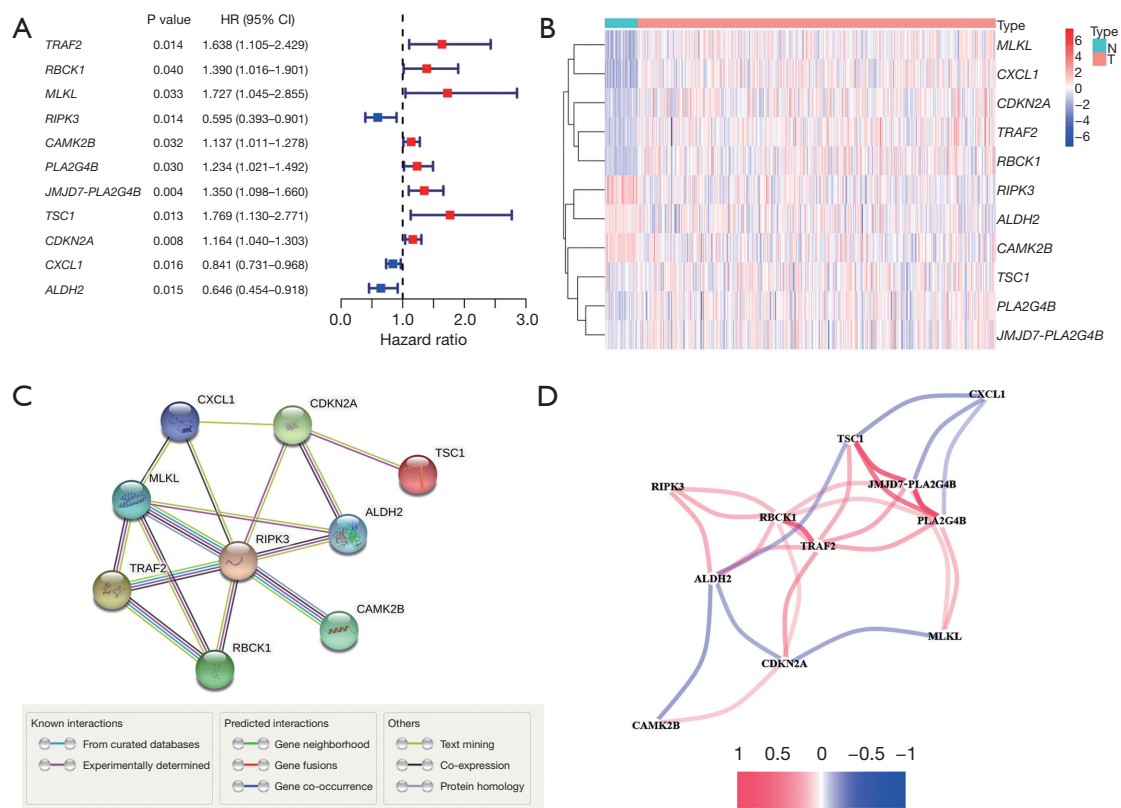Overall survival (OS) differences between the two groups

Figure 2 Identification of prognosis-related DENRGs. (A,B) The forest and heat map of 11 prognosis-related DENRGs were obtained using univariate Cox regression analysis. The data shows that *RIPK3*, *CXCL1* and *ALDH2* are highly expressed in normal tissues as protective genes (HR <1), while others are the risk genes (HR >1). (C,D) The PPI and correlation networks of prognosis-related DENRGs show that *RIPK3* and *MLKL* are the hub genes. DENRGs, differentially expressed necroptosis-related genes; HR, hazard ratio; PPI, protein-protein interaction; N, normal tissue; T, tumor tissue; CI, confidence interval.

were analyzed using the log-rank test. In addition, the ssGSEA scores were compared with the Mann-Whitney test. Data analyses were conducted with packages within R (version 4.0.4). The P<0.05 was the significance threshold.

Results

Identification of prognosis-related NRGs

We extracted 161 NRGs from 455 samples (38 normal and 417 COAD tissues) in the TCGA database and screened 118 DENRGs (table available at https://cdn.amegroups.cn/static/public/tcr-23-494-2.pdf). Then, 11 prognosis-related DENRGs were screened by univariate Cox regression analysis and showed in dendrogram (*Figure 2A*). *RIPK3*, *CXCL1* and *ALDH2* were the protective genes (HR <1), while others were the risk genes (HR >1). The heat map showed the expression of 11 prognosis-related DENRGs

in normal and tumor tissues (*Figure 2B*). Similar to the dendrogram, *RIPK3*, *CXCL1* and *ALDH2* were highly expressed in normal tissues. The PPI network showed that *RIPK3* and *MLKL*, which were strongly corrected with other genes, were the hub genes (*Figure 2C*). In addition, we performed an analysis for the correlation of these genes (*Figure 2D*).

Construction of the NRG prognostic signature

The 11 prognosis-related DENRGs were then subjected to an OS-based Lasso-penalized Cox regression analysis (*Figure 3A*). When 8 NRGs were gathered, the regression model reached the optimal ability (*Figure 3B*). To quantify the signature: risk score = $(\mathrm{Exp}_{TRAF2} \times 0.0086) + (\mathrm{Exp}_{RBCK1} \times 0.0020) + (\mathrm{Exp}_{MLKL} \times 0.0302) - (\mathrm{Exp}_{RIPK3} \times 0.0394) + (\mathrm{Exp}_{CAMK2B} \times 0.3044) + (\mathrm{Exp}_{JMJD7\text{-}PLA2G4B} \times 0.1854) +$
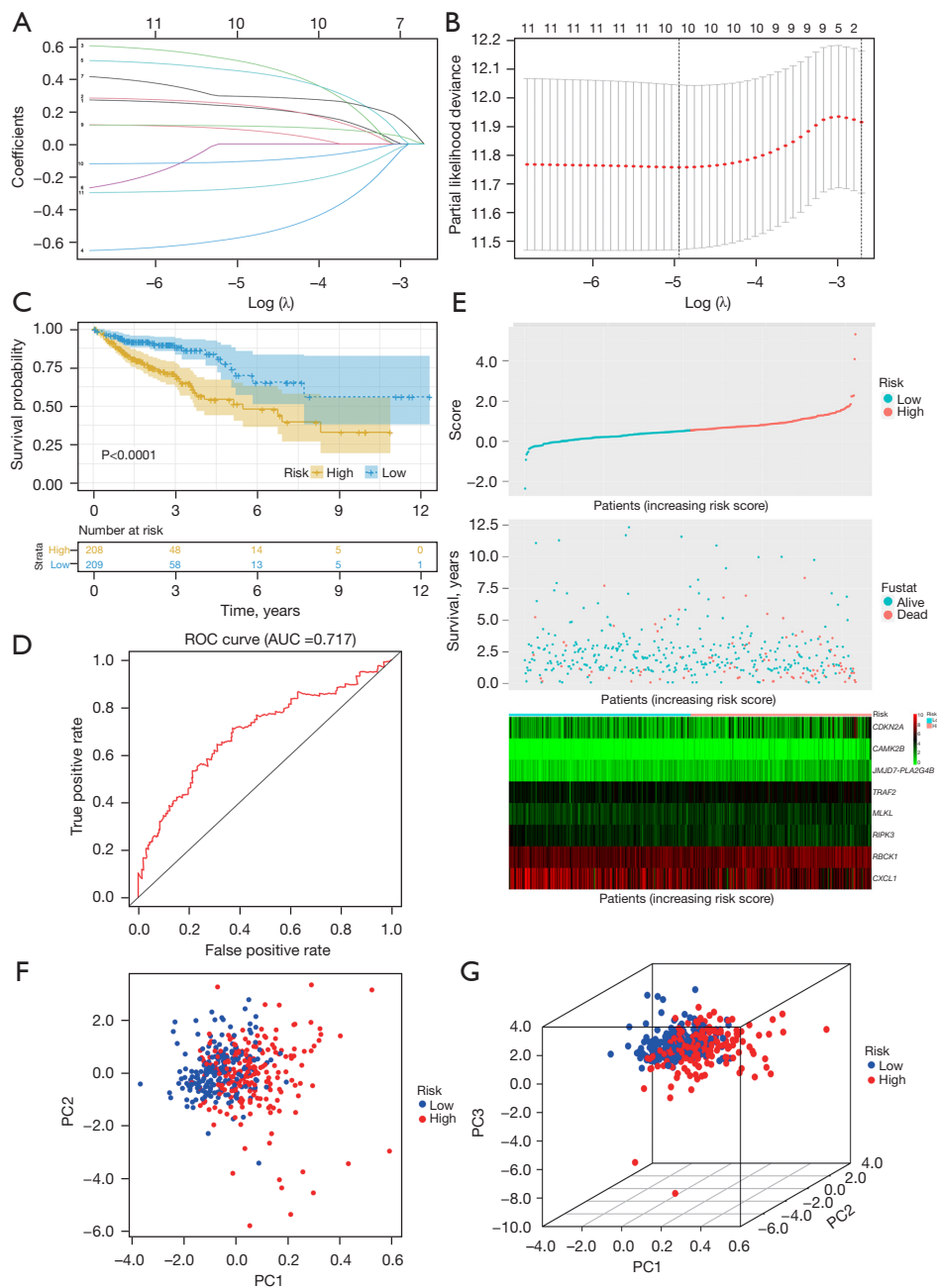
Figure 3 Construction of the NRG prognostic signature in TCGA-COAD dataset. (A) Distribution of Lasso coefficients of the 11 NRGs in TCGA-COAD dataset. (B) The generated coefficient distribution plots for the logarithmic (lambda) sequence for the selection of the best parameter (lambda). An optimal log lambda value is indicated by the vertical black line in the plot. (C) Kaplan-Meier survival curves between high- and low-risk groups based on prognostic signature in TCGA-COAD dataset, which show patients in the high-risk group have significantly worse OS than the low-risk group (P<0.0001). (D) The ROC curves analysis for survival prediction, and the AUC value (0.717) suggest that the signature have good predictability. (E) Prognostic classifier analyses (risk scores, survival status and genes expression) in distinguishing TCGA-COAD patients into low- and high-risk groups, which are presented in the order of increasing risk score. (F,G) 2D and 3D visualization of PCA based on signature in TCGA-COAD, which show low- and high-groups of patients cluster in different dimensions. ROC, receiver operating characteristic; AUC, area under the curve; PC, principal component; NRG, necroptosis-related gene; TCGA, The Cancer Genome Atlas; COAD, colon adenocarcinoma; OS, overall survival; 2D, two-dimensional; 3D, three-dimensional; PCA, principal component analysis.

$(Exp_{CDKN2A} \times 0.0077) - (Exp_{CXCL1} \times 0.0006)$. Next, the patients in TCGA-COAD were divided into low- and high-risk groups (table available at https://cdn.amegroups. cn/static/public/tcr-23-494-3.pdf). Kaplan-Meier analysis showed that patients in the high-risk group had significantly worse OS than the low-risk group (*Figure 3C*). Finally, the ROC curve was constructed to evaluate the 3-year prediction ability of the signature, and the area under the curve (AUC) value (0.717) indicated that the signature had good predictability (*Figure 3D*). The risk scores, survival status and NRGs expression of both groups were plotted by scatter plot and heat map (*Figure 3E*). In addition, PCA proved that two groups of patients clustered in different dimensions (*Figure 3F,3G*).

Validation of the NRG prognostic signature

To verify the stability of the constructed signature, we chose the GSE39582 dataset for testing. Similar to the TCGA-COAD dataset, patients in GSE39582 were divided into low- and high-risk groups (table available at https://cdn.amegroups.cn/static/public/tcr-23-494-4.pdf). Kaplan-Meier analysis showed that patients in the high-risk group had significantly worse OS (*Figure 4A*). The AUC value (0.617) of the ROC curve also indicated the good predictability (*Figure 4B*). The prognostic classifier analyses (risk scores, survival status and NRGs expression) were shown in *Figure 4C*. PCA also showed a dimensional difference between the two groups (*Figure 4D,4E*).

Independent prognostic analysis and construction of nomogram

We investigated the associations between NRGs and clinical characteristics in TCGA-COAD and GSE39582 datasets. First, we used heat map to show their correlation (red represented P<0.05), and found that these NRGs were strongly associated with the tumor stage (*Figure 5A*). This implied that the signature might be used to assess the tumor progression. Next, we investigated the independence of the signature in predicting patient prognosis. According to univariate and multivariate Cox regression analysis in TCGA-COAD and GSE39582 datasets, we found that the age, tumor stage, and risk score could assess COAD patient prognosis independently (P<0.05) (*Figure 5B-5E*). Finally, since multiple factors influence COAD development, we proposed a nomogram (C-index =0.772) for individualized assessment (*Figure 5F*). In addition, as predicted, the

HPA database had high expression of *JMJD7-PLA2G4B*, *CDKN2A*, *CAMK2B*, and *TRAF2* in COAD tissues (*Figure 5G*).

Genetic mutation and functional enrichment analysis of NRGs

We analyzed the genetic variation landscape of 8 NRGs in the signature. SNVs were detected in 32 of 56 (57.14%) COAD samples, and *JMJD7-PLA2G4B* had the highest mutation frequency (*Figure 6A*). In addition, missense mutation and single nucleotide polymorphisms (SNP) were the most common variant. C>T was the main SNV class (*Figure 6B*). For CNV analysis, the copy number of *CAMK2B* and *TRAF2* were amplified, while *RBCK1*, *JMJD7-PLA2G4B*, *CDKN2A*, *RIPK3*, and *MLKL* were deleted (*Figure 6C*). *Figure 6D* shows the location of CNV variation on the chromosome. Next, we analyzed the biological functions of these genes. The GO analysis indicated that "signal transduction", "cytosol" and "protein binding" were the main enriched characteristics (*Figure 7A*). While the KEGG analysis showed that "necroptosis" was the main enriched pathway (*Figure 7B*).

Gene set enrichment analysis

We analyzed the potential enrichment differences between the two groups by GSEA. We found that "citrate cycle TCA cycle", "valine leucine and isoleucine degradation", "peroxisome", "butanoate metabolism", "oxidative phosphorylation", "fatty acid metabolism" and "adipogenesis" were enriched in the low-risk group, while "mitotic spindle" was enriched in the high-risk group (*Figure 8*).

Immunological characteristics of NRGs

Given the close association between necroptosis and immunity, we analyzed the immunological characteristics of the two groups by ssGSEA. Immune cells [DCs, neutrophils, natural killer (NK) cells, Th2 cells and regulatory T cell (Treg)] and immunological function [antigen presenting cell (APC) co-inhibition and parainflammation] showed significant differences in both two datasets (*Figure 9A-9D*). Furthermore, we predicted the possible immune checkpoints and obtained 10 potential therapeutic targets (*ANGPTL7*, *BTN1A1*, *BTNL9*, *CD276*, *ICOSLG*, *NCR3LG1*, *NECTIN1*, *PVR*, *PVRIG* and *SIRPA*) (*Figure 9E*).
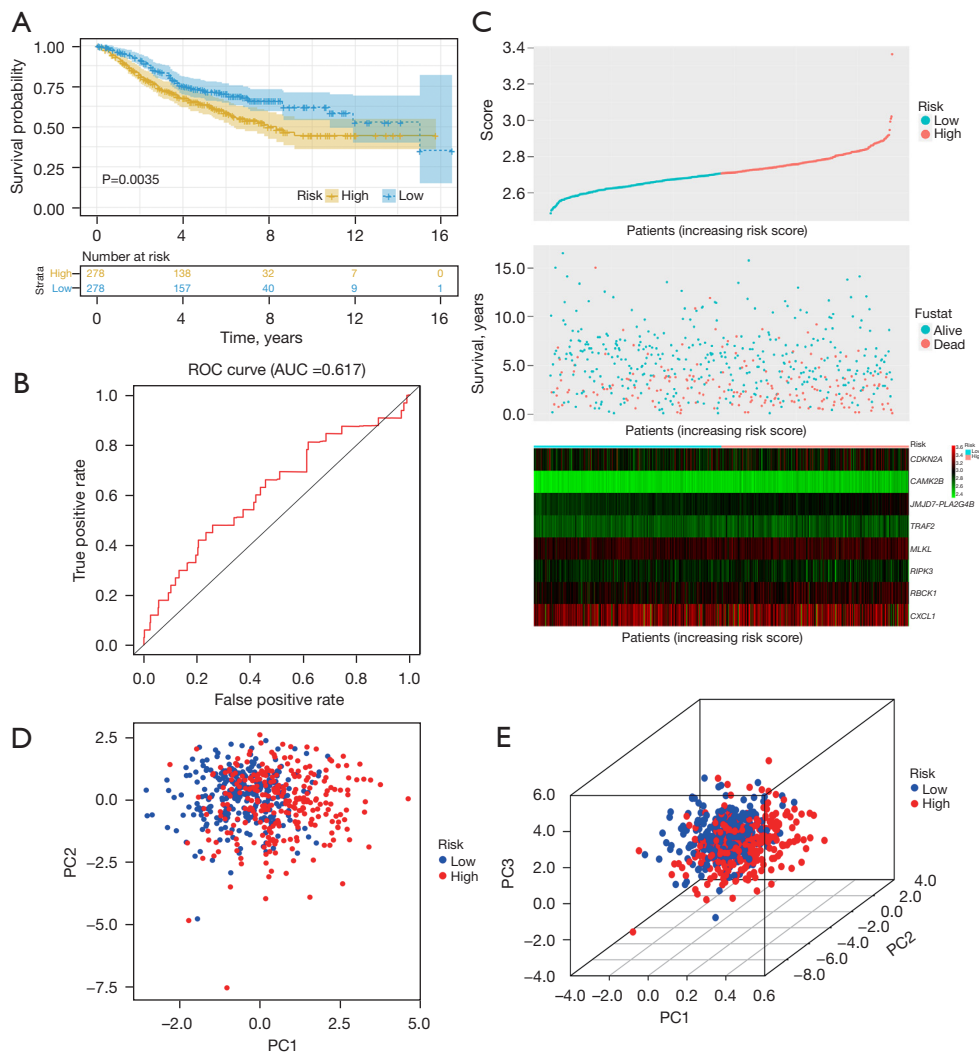
Figure 4 Validation of the necroptosis-related gene prognostic signature in GSE39582 dataset. (A) Kaplan-Meier survival curves between high- and low-risk groups based on prognostic signature in GSE39582 dataset, which show patients in the high-risk group have significantly worse OS than the low-risk group (P=0.0035). (B) The ROC curves analysis for survival prediction, and the AUC value (0.617) suggest that the signature have good predictability. (C) Prognostic classifier analyses (risk scores, survival status and genes expression) in distinguishing GSE39582 patients into low- and high-risk groups, which are presented in the order of increasing risk score. (D,E) 2D and 3D visualization of PCA based on signature in GSE39582, which show low- and high-groups of patients cluster in different dimensions. ROC, receiver operating characteristic; AUC, area under the curve; PC, principal component; OS, overall survival; 2D, two-dimensional; 3D, three-dimensional; PCA, principal component analysis.

Discussion

COAD is a common gastrointestinal tumor that affects the OS of patients due to its insidious onset and high recurrence rate (3). The prognosis situation of COAD still plagues physicians and patients. Currently, cancer development is mainly categorized by the Tumor Node Metastasis (TNM) system internationally. However, for COAD with high heterogeneity, the traditional TNM system cannot effectively predict the prognosis of these patients. Therefore, it is necessary to propose new biomarkers for an individualized clinical assessment of the prognosis in COAD patients. Necroptosis influences tumor development by modulating the microenvironment and the
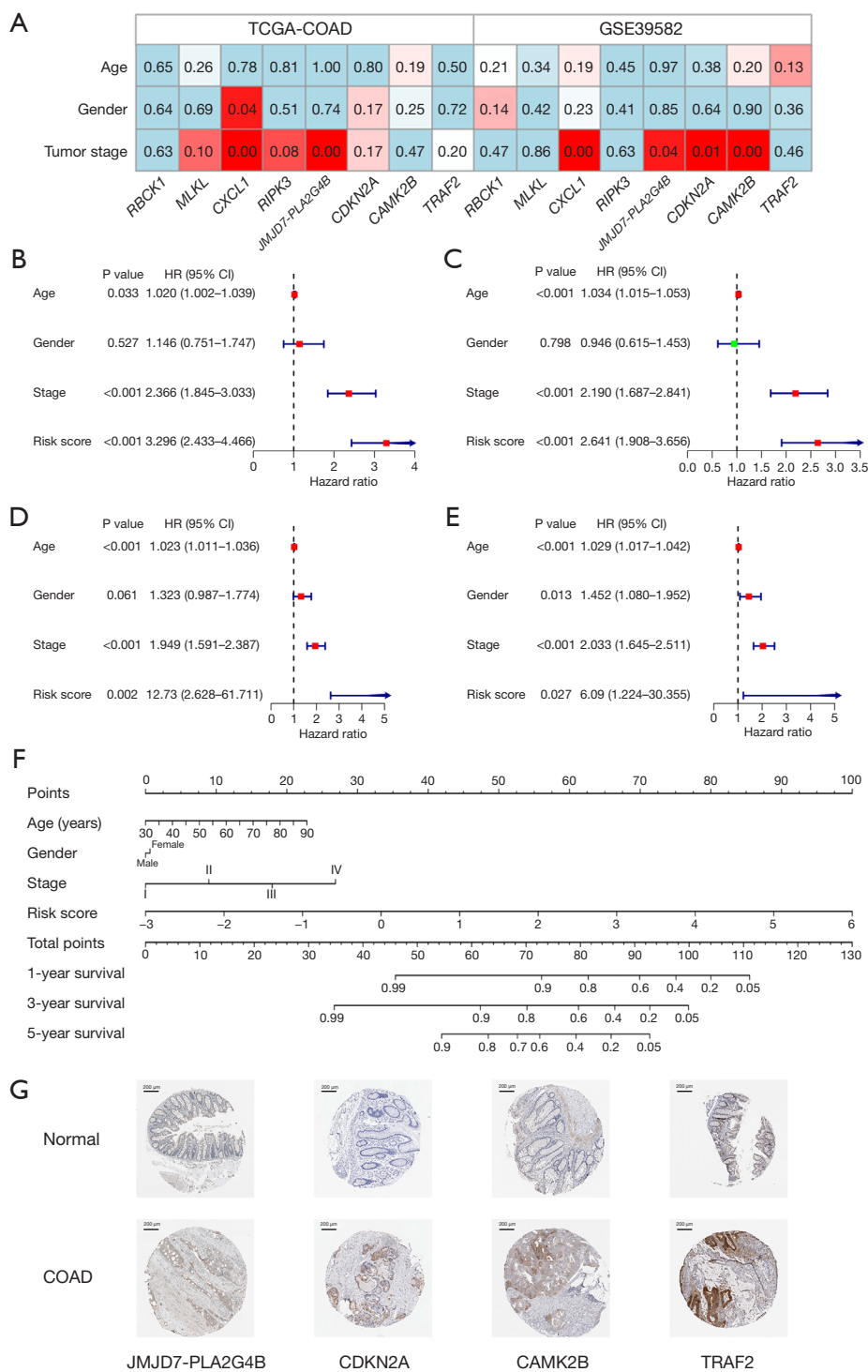
Figure 5 Clinical significance of the NRG prognostic signature. (A) Correlation of NRGs with clinical characteristics in TCGA-COAD and GSE39582 datasets. The heat map shows the expression of NRGs in the two datasets is significantly correlated with tumor stage (P<0.05). (B,C) Univariate and multivariate Cox regression analysis of clinical characteristics and the signature-based risk score in TCGA-COAD dataset, which show the independence of the signature in predicting patient prognosis (P<0.05). (D,E) Univariate and multivariate Cox regression analysis of clinical characteristics and the signature-based risk score in GSE39582 dataset, which show the independence of

Transl Cancer Res 2023;12(9):2239-2255 | https://dx.doi.org/10.21037/tcr-23-494

the signature in predicting patient prognosis (P<0.05). (F) Construction of a signature-based nomogram to predict COAD prognosis. (G) The immunohistochemistry images of *JMJD7-PLA2G4B* (https://www.proteinatlas.org/ENSG00000168970-JMJD7-PLA2G4B/tissue/colon; https://www.proteinatlas.org/ENSG00000168970-JMJD7-PLA2G4B/pathology/colorectal+cancer#img), *CDKN2A* (https://www.proteinatlas.org/ENSG00000147889-CDKN2A/tissue/colon; https://www.proteinatlas.org/ENSG00000147889-CDKN2A/pathology/colorectal+cancer#img), *CAMK2B* (https://www.proteinatlas.org/ENSG00000058404-CAMK2B/tissue/colon; https://www.proteinatlas.org/ENSG00000058404-CAMK2B/pathology/colorectal+cancer#img) and *TRAF2* (https://www.proteinatlas.org/ENSG00000127191-TRAF2/tissue/colon; https://www.proteinatlas.org/ENSG00000127191-TRAF2/pathology/colorectal+cancer#img) in normal and COAD tissues reveal that the expression of these genes was increased in tumor tissue. TCGA, The Cancer Genome Atlas; COAD, colon adenocarcinoma; HR, hazard ratio; CI, confidence interval; NRGs, necroptosis-related genes.
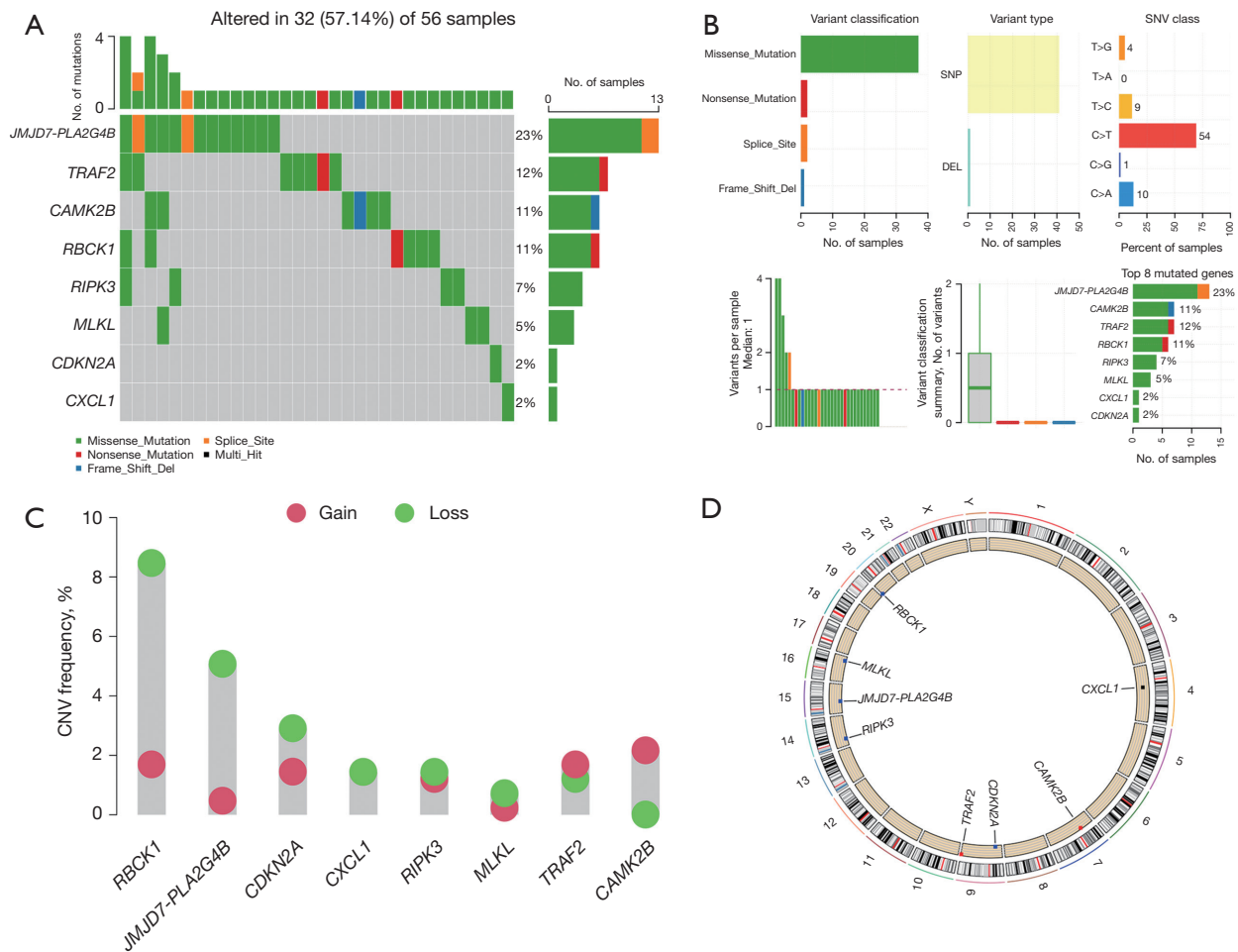

Figure 6 The landscape of genetic mutation in the NRG prognostic signature. (A,B) The mutation frequency and classification of NRGs in COAD, which show the *JMJD7-PLA2G4B* has the highest mutation frequency and C>T is the main SNV class. (C) The CNV frequency of NRGs in COAD, and the height of the column represented the alteration frequency. (D) The location of CNV variation on the chromosome. SNP, single nucleotide polymorphisms; DEL, deletion; SNV, simple nucleotide variation; No., number; CNV, copy number variation; NRG, necroptosis-related gene; COAD, colon adenocarcinoma.
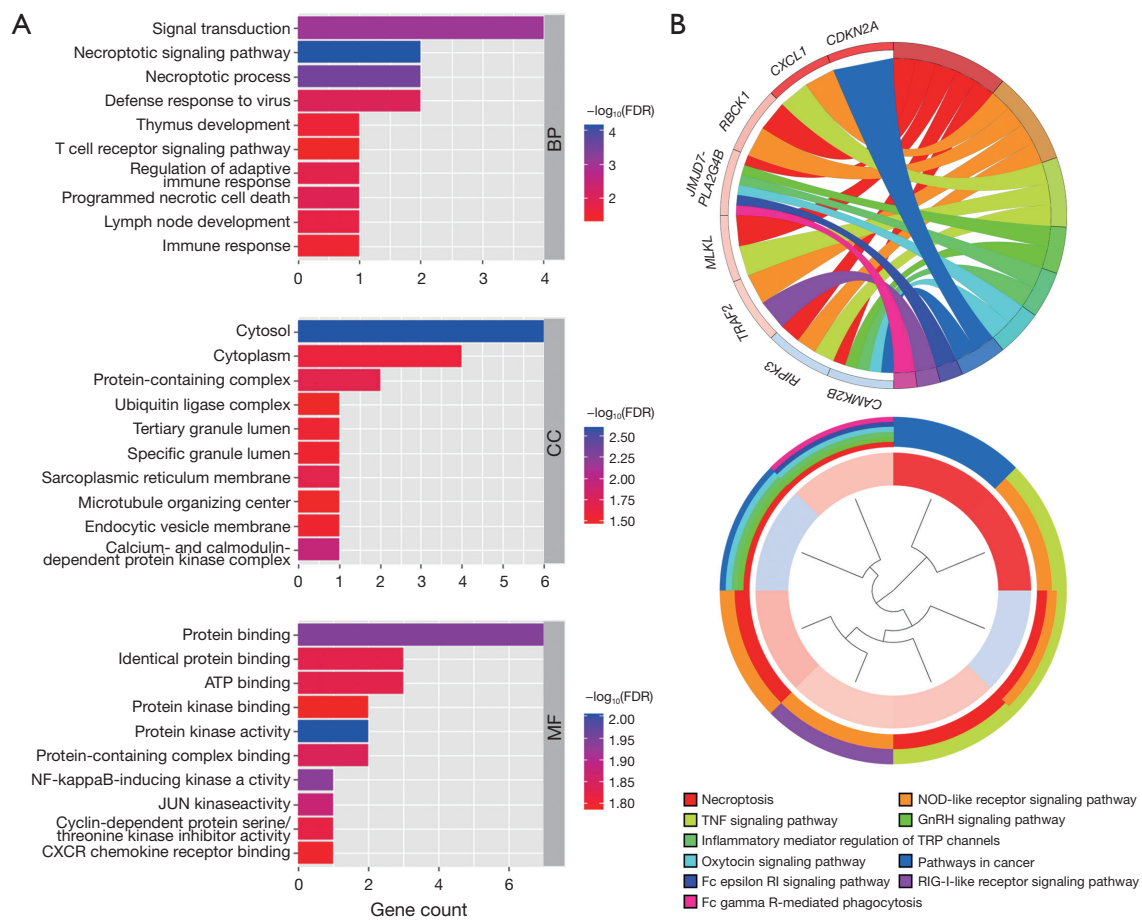
Figure 7 The functional enrichment analyses of NRGs in prognostic signature. (A) GO analysis of NRGs show "signal transduction" (BP), "cytosol" (CC) and "protein binding" (MF) are the main enriched characteristics. (B) KEGG pathways analysis of NRGs show that "necroptosis" is the main enriched pathway. BP, biological process; CC, cellular component; MF, molecular function; FDR, false discovery rate; ATP, adenosine triphosphate; NF, nuclear factor; CXCR, CXC chemokine receptor; TNF, tumor necrosis factor; TRP, transient receptor potential; NOD, nucleotide-binding and oligomerization domain; GnRH, gonadotropin-releasing hormone; RIG-I, retinoic acid-inducible gene I; NRGs, necroptosis-related genes; GO, Gene Ontology; KEGG, Kyoto Encyclopedia of Genes and Genomes.

immune response (27). Several genes have been identified to regulate the necroptosis in COAD (28-30). Oliver Metzig *et al.* found that 5-fluorouracil induced necroptosis in colorectal cancer at the cellular level (31). However, the association between necroptosis and prognosis has not been reported. Here, we analyzed the NRGs in COAD patients and constructed a prognostic signature for individualized assessment of these patients' prognosis. Furthermore, we proposed potential immunotherapeutic targets of COAD using immunological analysis.

Necroptosis, mediated by *RIPK3* and its substrate *MLKL*, is the best-characterized form of regulated necrosis. Compared with cell contraction and nuclear fragmentation

during apoptosis, necrotic apoptosis shows organelles swelling, cellular membrane rupture, and translucent cytoplasm (32). Extracellular and intracellular signals are capable of inducing cell necrosis. Among them, TNFR1 is a classical signal transduction pathway mediating cell necroptosis. Moreover, necroptosis is involved in regulating several signaling pathways, including caspase-8-dependent apoptosis, NF-κB-dependent inflammation, and MAP kinase cascade (33). Therefore, necroptosis plays an important role in maintaining the physiological machinery. Furthermore, recent studies have revealed that necroptosis plays a key role in various clinical diseases. Importantly, targeting necroptosis can be a potential therapeutic
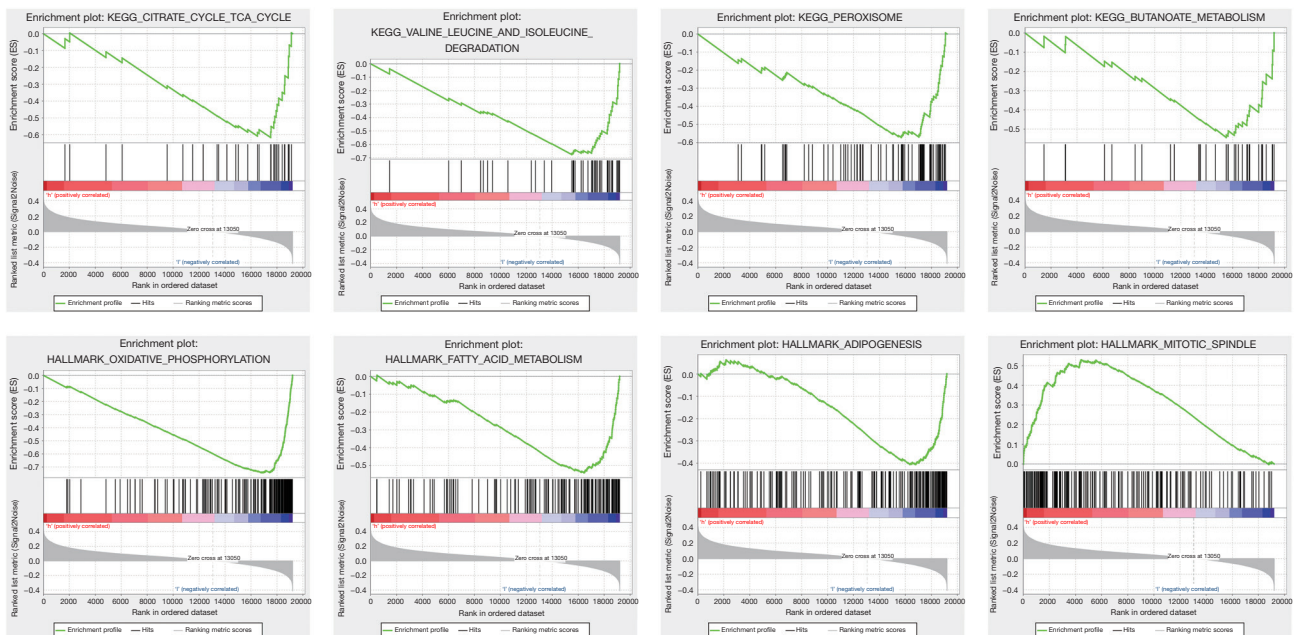
Figure 8 Gene set enrichment analysis of low- and high-risk groups based on the necroptosis-related gene prognostic signature. The analysis show that "citrate cycle TCA cycle", "valine leucine and isoleucine degradation", "peroxisome", "butanoate metabolism", "oxidative phosphorylation", "fatty acid metabolism" and "adipogenesis" are enriched in the low-risk group, while "mitotic spindle" is enriched in the high-risk group. KEGG, Kyoto Encyclopedia of Genes and Genomes; TCA, tricarboxylic acid.

modality for multiple diseases.

We analyzed the expression of NRGs between normal and COAD samples and found that the majority (118 of 161) of these NRGs had significant expression differences. We identified 11 NRGs associated with OS, including necroptosis key genes *RIPK3* and *MLKL*. These findings suggest that necroptosis plays an important role in the survival status of COAD patients. Further, we searched representative genes by Lasso-penalized Cox regression analysis to improve the interpretability and predictivity of the prognostic signature. Finally, we constructed a prognostic signature containing 8 NRGs. The *RIPK3*, *MLKL*, and the other genes, including *TRAF2*, *CXCL1*, *RBCK1*, *CDKN2A*, *JMJD7-PLA2G4B*, and *CAMK2B*, participated in constructing the signature. These genes have been reported in several cancers (34-51), some of which have been confirmed to affect the occurrence of COAD directly or indirectly (*Table 3*). This observation suggests the correlation and accuracy of the prognostic signature. Moreover, it provides some new targets for the treatment of COAD.

To verify the accuracy of the constructed signature, we selected two independent datasets of TCGA-COAD and GSE39582. PCA showed that patients in two group clusters were separated with different dimensions, confirming the high specificity of the signature. Kaplan-Meier analysis demonstrated the poor prognosis of patients in the high-risk group. The AUC values in ROC curves were 0.717 (TCGA-COAD) and 0.617 (GSE39582), exhibiting good predictive ability. In addition, we found that the gene expression in the signature was closely related to the tumor stage. This implied its feasibility in assessing the COAD progression. Furthermore, we demonstrated the independence of prognostic features in predicting prognosis in COAD. Overall, the constructed prognostic signature in our study has great clinical application.

Given the heterogeneity of tumorigenesis, a single variable cannot accurately predict a patient's prognosis. Therefore, we constructed a nomogram containing clinical characteristics (age, gender, and tumor stage) and the risk score to solve this problem. The C-index of the nomogram was 0.772, implying good predictive performance. Thus, this nomogram had great potential for individualized assessment of the COAD patients' prognosis.

Next, we attempted enrichment analysis for their biological functions. GO analysis showed that the "signal transduction" and "necroptosis related processes" were
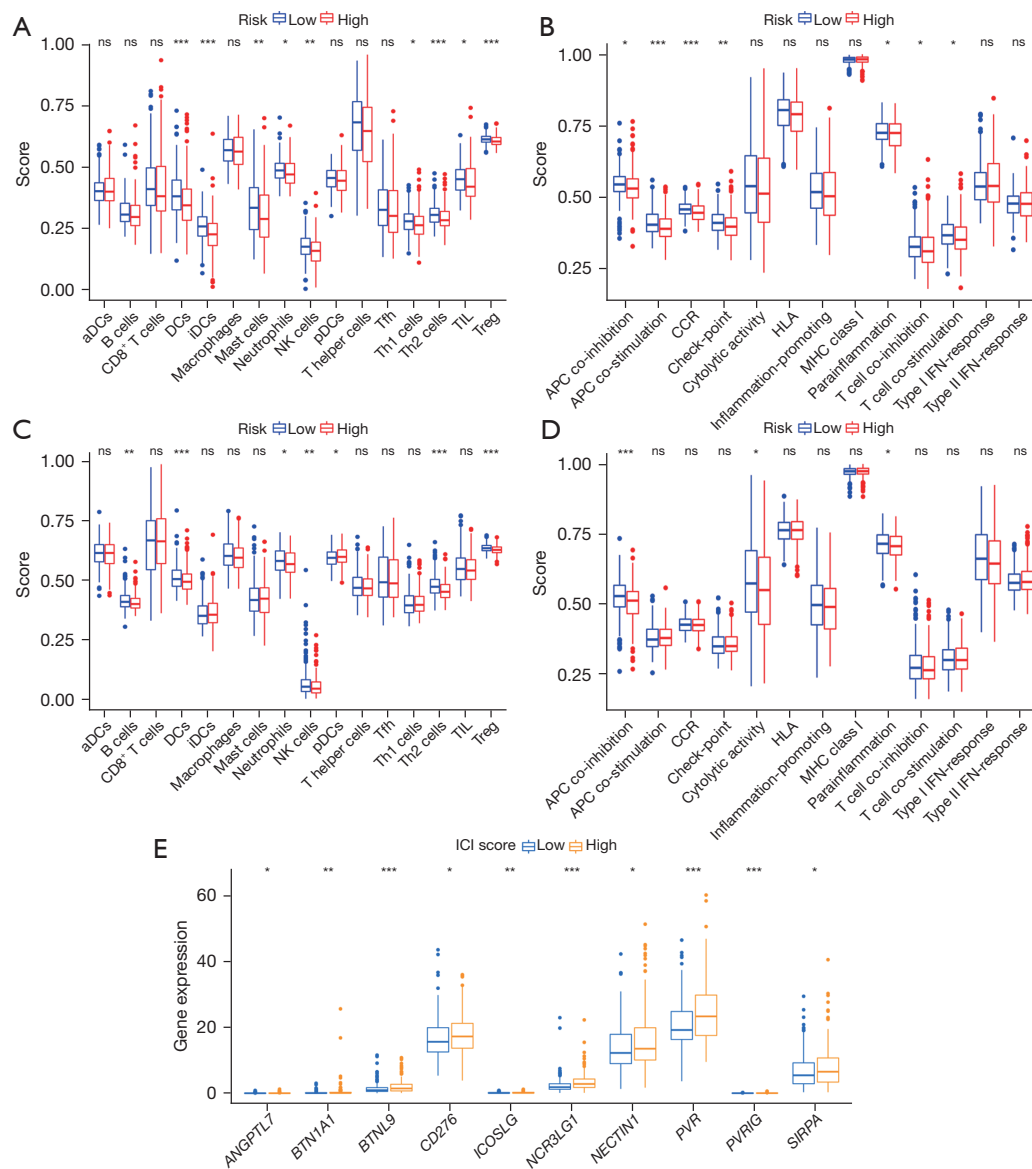
Figure 9 Immunologic characteristics of the necroptosis-related gene prognostic signature. (A) Boxplots of the correlations between the scores of 16 immune cells and risk groups in TCGA-COAD dataset, which show significant differences in DCs, iDCs, mast cells, neutrophils, NK cells, Th1 cells, Th2 cells, TIL and Treg between the two groups. (B) Boxplots of the correlations between the scores of 13 immune-related functions and risk groups in TCGA-COAD dataset, which show significant differences in APC co-inhibition, APC co-stimulation, CCR, check point, parainflammation, T cell co-inhibition and T cell co-stimulation between the two groups. (C) Boxplots of the correlations between the scores of 16 immune cells and risk groups in GSE39582 dataset, which show significant differences in B cells, DCs, neutrophils, NK cells, pDCs, Th2 cells and Treg between the two groups. (D) Boxplots of the correlations between the scores of 13 immune-related functions and risk groups in GSE39582 dataset, which show significant differences in APC co-inhibition, cytolytic activity, parainflammation between the two groups. (E) Boxplots of immune checkpoints expression of two groups, which show *ANGPTL7*, *BTN1A1*, *BTNL9*, *CD276*, *ICOSLG*, *NCR3LG1*, *NECTIN1*, *PVR*, *PVRIG* and *SIRPA* are potential therapeutic targets. ns, no significance; *, P<0.05; **, P<0.01; ***, P<0.001. aDC, activated dendritic cell; DCs, dendritic cells; iDCs, immature dendritic cells; NK, natural killer; pDCs, plasmacytoid dendritic cells; Tfh, follicular helper T cell; Th, helper T; TIL, tumor infiltrating lymphocyte; Treg, regulatory T cell; APC, antigen-presenting cells; CCR, C-C chemokine receptor; HLA, human leukocyte antigen; MHC, major histocompatibility complex; IFN, interferon; ICI, immune checkpoint inhibitor; TCGA, The Cancer Genome Atlas; COAD, colon adenocarcinoma.

Table 3 The mechanism of action and function of NRGs in cancer

NRGs	Mechanism of action and function	Cancer type	References
RIPK3	*RIPK3* is a key factor that constitutes the necrotic bodies and initiates the necroptosis pathways. The anti-tumor activity of *RIPK3* may be related to its mediated TRIM28 phosphorylation	Prostate cancer; lung cancer; colon cancer	(34-39)
MLKL	As an executioner, *MLKL* plays an essential role in necroptosis. *MLKL* is activated by *RIPK3* and prompts membrane rupture, which induces necroptosis	Melanoma; colon cancer; lymphoma	(30,40,41)
TRAF2	*TRAF2* is a suppressor of necroptosis and maintains tissue organ homeostasis	Hepatocarcinoma	(42,43)
CXCL1	*CXCL1* is critical for pre-metastatic niche formation and metastasis	Colon cancer	(44,45)
RBCK1	*RBCK1* plays an important role in PKC-dependent cell growth	Renal cancer; breast cancer; colon cancer	(46-48)
CDKN2A	*CDKN2A* is a tumor suppressor, which may be mediated by the ILF3-AS1/EZH2/H3K27me3/CDKN2A pathway	Colon cancer	(49)
JMJD7-PLA2G4B	*JMJD7-PLA2G4B* promotes the progression of head and neck carcinoma by activating AKT	Head and neck carcinoma	(50)
CAMK2B	*CAMK2B* is the core effector molecule in regulating the tumor microenvironment	Renal carcinoma	(51)

NRGs, necroptosis-related genes; PKC, protein kinase C.

the main enriched processes. Furthermore, these genes were associated with immune processes, including "thymus development", "T cell receptor signaling pathway" and "immune response". KEGG analysis revealed that "necroptosis" was the main enriched pathway. In addition, nucleotide-binding and oligomerization domain (NOD)-like receptor and TNF signaling pathways were also significantly enriched. Of note, these pathways are also involved in the regulation of necroptosis. The TNF pathway is a key initiator of necroptosis (52). While NOD-like receptor signaling pathway can also induce necroptosis (53). KEGG analysis also revealed immune related enrichment ("Fc epsilon RI signaling pathway", "RIG-I-like receptor signaling pathway", and "Fc gamma R-mediated phagocytosis"). In addition, we explored the differential enrichment of NRGs between the two groups by GSEA. We found that mitochondrial metabolic pathways were enriched in the low-risk group, implying that disrupting intracellular metabolic pathways may significantly contribute to the poor prognosis. Thus, NRGs in the signature may be the main reason affecting the cellular metabolic pathways.

Necroptosis is critically involved in immune processes (54). Therefore, we assessed differences in immune characteristics between the two groups by ssGSEA. We found that the differences in immune cells were mainly concentrated in the low-risk group. The DCs, neutrophils, NK cells, Th2 cells, and Treg presented apparent differences in

both datasets. In addition, immunologic functions showed similar results in the two datasets. These results implied that the poor OS of COAD might be related to the destruction of the immune function, in which the decrease of APC co-inhibition and parainflammation were the main reasons. Acute exposure to DAMPs can prime anti-tumour immunity by activating APC and then destroying tumor cells (55). However, APC co-inhibition reduces this immune response, affecting the OS of patients. In addition, the parainflammation induced by necroptosis can inhibit tumour cell development via maintenance of growth arrest and immune clearance of the senescent cells (56). Immune checkpoints overexpression is one of the causes of tumor progression and is used to treat COAD (57). Snyder *et al.* showed that combining necroptosis with immune checkpoints could synergistically improve anti-tumor immunity (58). Therefore, we screened possible immune checkpoints to provide novel targets for COAD treatment.

Our study had some limitations. First, the present study was retrospective. Thus, more samples are required in the future to further validate these results. We focus on collecting relevant cases for future clinical treatment and constructing a database for validation. In addition, we will also explore the situation of necroptosis after neoadjuvant chemotherapy and attempt to find new therapeutic targets for COAD. Secondly, this study was based on database

analysis. Hence, the further proteomic examination is needed to validate the results in the future. Finally, the potential molecular mechanisms and the selection of therapeutic targets need to be investigated further by combining clinical testing and biological cytology.

Conclusions

In conclusion, we systematically analyzed the relationship of NRGs expression with COAD. As a result, we constructed a prognostic signature containing 8 NRGs and a nomogram with individualized clinical practical value. In addition, we proposed potential therapeutic targets through immunological analysis, which provided the breakthrough for COAD treatment.

Acknowledgments

Footnote

Reporting Checklist: The authors have completed the TRIPOD reporting checklist. Available at https://tcr. amegroups.com/article/view/10.21037/tcr-23-494/rc

Peer Review File: Available at https://tcr.amegroups.com/ article/view/10.21037/tcr-23-494/prf

Conflicts of Interest: All authors have completed the ICMJE uniform disclosure form (available at https://tcr.amegroups. com/article/view/10.21037/tcr-23-494/coif). The authors have no conflicts of interest to declare.

Ethical Statement: The authors are accountable for all aspects of the work in ensuring that questions related to the accuracy or integrity of any part of the work are appropriately investigated and resolved. The study was conducted in accordance with the Declaration of Helsinki (as revised in 2013).

Open Access Statement: This is an Open Access article distributed in accordance with the Creative Commons Attribution-NonCommercial-NoDerivs 4.0 International License (CC BY-NC-ND 4.0), which permits the non-commercial replication and distribution of the article with the strict proviso that no changes or edits are made and the original work is properly cited (including links to both the formal publication through the relevant DOI and the license). See: https://creativecommons.org/licenses/by-nc-nd/4.0/.

References

1. Siegel RL, Wagle NS, Cercek A, et al. Colorectal cancer statistics, 2023. CA Cancer J Clin 2023;73:233-54.
2. Fabregas JC, Ramnaraign B, George TJ. Clinical Updates for Colon Cancer Care in 2022. Clin Colorectal Cancer 2022;21:198-203.
3. Siegel RL, Miller KD, Fuchs HE, et al. Cancer statistics, 2022. CA Cancer J Clin 2022;72:7-33.
4. Altieri MS, Thompson H, Pryor A, et al. Incidence of colon resections is increasing in the younger populations: should an early initiation of colon cancer screening be implemented? Surg Endosc 2021;35:3636-41.
5. Islami F, Ward EM, Sung H, et al. Annual Report to the Nation on the Status of Cancer, Part 1: National Cancer Statistics. J Natl Cancer Inst 2021;113:1648-69.
6. Abdel-Rahman O, Karachiwala H, Koski S. Patterns of colorectal cancer diagnosis among younger adults in a real-world, population-based cohort. Future Oncol 2022;18:47-54.
7. Hossain MS, Karuniawati H, Jairoun AA, et al. Colorectal Cancer: A Review of Carcinogenesis, Global Epidemiology, Current Challenges, Risk Factors, Preventive and Treatment Strategies. Cancers (Basel) 2022;14:1732.
8. Song M, Chan AT, Sun J. Influence of the Gut Microbiome, Diet, and Environment on Risk of Colorectal Cancer. Gastroenterology 2020;158:322-40.
9. Gately L, Jalali A, Semira C, et al. Stage dependent recurrence patterns and post-recurrence outcomes in non-metastatic colon cancer. Acta Oncol 2021;60:1106-13.
10. Degterev A, Huang Z, Boyce M, et al. Chemical inhibitor of nonapoptotic cell death with therapeutic potential for ischemic brain injury. Nat Chem Biol 2005;1:112-9.
11. Tang R, Xu J, Zhang B, et al. Ferroptosis, necroptosis, and pyroptosis in anticancer immunity. J Hematol Oncol 2020;13:110.
12. Zhou H, Liu L, Ma X, et al. RIP1/RIP3/MLKL-mediated necroptosis contributes to vinblastine-induced myocardial damage. Mol Cell Biochem 2021;476:1233-43.
13. Hu X, Xu Y, Zhang H, et al. Role of necroptosis in

traumatic brain and spinal cord injuries. J Adv Res 2022;40:125-34.

14. Lei XY, Tan RZ, Jia J, et al. Artesunate relieves acute kidney injury through inhibiting macrophagic Mincle-mediated necroptosis and inflammation to tubular epithelial cell. J Cell Mol Med 2021;25:8775-88.

15. Markowitsch SD, Juetter KM, Schupp P, et al. Shikonin Reduces Growth of Docetaxel-Resistant Prostate Cancer Cells Mainly through Necroptosis. Cancers (Basel) 2021;13:882.

16. Ding Y, He C, Lu S, et al. MLKL contributes to shikonin-induced glioma cell necroptosis via promotion of chromatinolysis. Cancer Lett 2019;467:58-71.

17. Liu T, Sun X, Cao Z. Shikonin-induced necroptosis in nasopharyngeal carcinoma cells via ROS overproduction and upregulation of RIPK1/RIPK3/MLKL expression. Onco Targets Ther 2019;12:2605-14.

18. Khing TM, Po WW, Sohn UD. Fluoxetine Enhances Anti-tumor Activity of Paclitaxel in Gastric Adenocarcinoma Cells by Triggering Apoptosis and Necroptosis. Anticancer Res 2019;39:6155-63.

19. Seifert L, Werba G, Tiwari S, et al. The necrosome promotes pancreatic oncogenesis via CXCL1 and Mincle-induced immune suppression. Nature 2016;532:245-9.

20. Liu X, Zhou M, Mei L, et al. Key roles of necroptotic factors in promoting tumor growth. Oncotarget 2016;7:22219-33.

21. Gao W, Wang X, Zhou Y, et al. Autophagy, ferroptosis, pyroptosis, and necroptosis in tumor immunotherapy. Signal Transduct Target Ther 2022;7:196.

22. Murai S, Shirasaki Y, Nakano H. Time-Lapse Imaging of Necroptosis and DAMP Release at Single-Cell Resolution. Methods Mol Biol 2021;2274:353-63.

23. Yang H, Jiang Q. A multi-omics-based investigation of the immunological and prognostic impact of necroptosis-related genes in patients with hepatocellular carcinoma. J Clin Lab Anal 2022;36:e24346.

24. Hu T, Zhao X, Zhao Y, et al. Identification and Verification of Necroptosis-Related Gene Signature and Associated Regulatory Axis in Breast Cancer. Front Genet 2022;13:842218.

25. He R, Zhang M, He L, et al. Integrated Analysis of Necroptosis-Related Genes for Prognosis, Immune Microenvironment Infiltration, and Drug Sensitivity in Colon Cancer. Front Med (Lausanne) 2022;9:845271.

26. Yi M, Nissley DV, McCormick F, et al. ssGSEA score-based Ras dependency indexes derived from gene expression data reveal potential Ras addiction mechanisms

with possible clinical implications. Sci Rep 2020;10:10258.

27. Gong Y, Fan Z, Luo G, et al. The role of necroptosis in cancer biology and therapy. Mol Cancer 2019;18:100.

28. Yu YQ, Thonn V, Patankar JV, et al. SMYD2 targets RIPK1 and restricts TNF-induced apoptosis and necroptosis to support colon tumor growth. Cell Death Dis 2022;13:52.

29. Kang JI, Hong JY, Choi JS, et al. Columbianadin Inhibits Cell Proliferation by Inducing Apoptosis and Necroptosis in HCT116 Colon Cancer Cells. Biomol Ther (Seoul) 2016;24:320-7.

30. D'Onofrio N, Martino E, Balestrieri A, et al. Diet-derived ergothioneine induces necroptosis in colorectal cancer cells by activating the SIRT3/MLKL pathway. FEBS Lett 2022;596:1313-29.

31. Oliver Metzig M, Fuchs D, Tagscherer KE, et al. Inhibition of caspases primes colon cancer cells for 5-fluorouracil-induced TNF-α-dependent necroptosis driven by RIP1 kinase and NF-κB. Oncogene 2016;35:3399-409.

32. Bertheloot D, Latz E, Franklin BS. Necroptosis, pyroptosis and apoptosis: an intricate game of cell death. Cell Mol Immunol 2021;18:1106-21.

33. Dai W, Cheng J, Leng X, et al. The potential role of necroptosis in clinical diseases (Review). Int J Mol Med 2021;47:89.

34. Feng X, Song Q, Yu A, et al. Receptor-interacting protein kinase 3 is a predictor of survival and plays a tumor suppressive role in colorectal cancer. Neoplasma 2015;62:592-601.

35. Liu S, Joshi K, Denning MF, et al. RIPK3 signaling and its role in the pathogenesis of cancers. Cell Mol Life Sci 2021;78:7199-217.

36. Park HH, Kim HR, Park SY, et al. RIPK3 activation induces TRIM28 derepression in cancer cells and enhances the anti-tumor microenvironment. Mol Cancer 2021;20:107.

37. Wang KJ, Wang KY, Zhang HZ, et al. Up-Regulation of RIP3 Alleviates Prostate Cancer Progression by Activation of RIP3/MLKL Signaling Pathway and Induction of Necroptosis. Front Oncol 2020;10:1720.

38. Park JH, Jung KH, Kim SJ, et al. HS-173 as a novel inducer of RIP3-dependent necroptosis in lung cancer. Cancer Lett 2019;444:94-104.

39. Cho E, Lee JK, Park E, et al. Antitumor activity of HPA3P through RIPK3-dependent regulated necrotic cell death in colon cancer. Oncotarget 2018;9:7902-17.

40. Martens S, Bridelance J, Roelandt R, et al. MLKL in

cancer: more than a necroptosis regulator. Cell Death Differ 2021;28:1757-72.

41. Van Hoecke L, Van Lint S, Roose K, et al. Treatment with mRNA coding for the necroptosis mediator MLKL induces antitumor immunity directed against neo-epitopes. Nat Commun 2018;9:3417.

42. Petersen SL, Chen TT, Lawrence DA, et al. TRAF2 is a biologically important necroptosis suppressor. Cell Death Differ 2015;22:1846-57.

43. Schneider AT, Gautheron J, Feoktistova M, et al. RIPK1 Suppresses a TRAF2-Dependent Pathway to Liver Cancer. Cancer Cell 2017;31:94-109.

44. Liu ZY, Zheng M, Li YM, et al. RIP3 promotes colitis-associated colorectal cancer by controlling tumor cell proliferation and CXCL1-induced immune suppression. Theranostics 2019;9:3659-73.

45. Wang D, Sun H, Wei J, et al. CXCL1 Is Critical for Premetastatic Niche Formation and Metastasis in Colorectal Cancer. Cancer Res 2017;77:3655-65.

46. Yu S, Dai J, Ma M, et al. RBCK1 promotes p53 degradation via ubiquitination in renal cell carcinoma. Cell Death Dis 2019;10:254.

47. Gustafsson N, Zhao C, Gustafsson JA, et al. RBCK1 drives breast cancer cell proliferation by promoting transcription of estrogen receptor alpha and cyclin B1. Cancer Res 2010;70:1265-74.

48. Liu ML, Zang F, Zhang SJ. RBCK1 contributes to chemoresistance and stemness in colorectal cancer (CRC). Biomed Pharmacother 2019;118:109250.

49. Hong S, Li S, Bi M, et al. lncRNA ILF3-AS1 promotes proliferation and metastasis of colorectal cancer cells by recruiting histone methylase EZH2. Mol Ther Nucleic Acids 2021;24:1012-23.

50. Cheng Y, Wang Y, Li J, et al. A novel read-through transcript JMJD7-PLA2G4B regulates head and neck squamous cell carcinoma cell proliferation and survival. Oncotarget 2017;8:1972-82.

51. Jia Q, Liao X, Zhang Y, et al. Anti-Tumor Role of CAMK2B in Remodeling the Stromal Microenvironment and Inhibiting Proliferation in Papillary Renal Cell Carcinoma. Front Oncol 2022;12:740051.

52. Pinci F, Gaidt MM, Jung C, et al. Tumor necrosis factor is a necroptosis-associated alarmin. Front Immunol 2022;13:1074440.

53. Zheng M, Kanneganti TD. The regulation of the ZBP1-NLRP3 inflammasome and its implications in pyroptosis, apoptosis, and necroptosis (PANoptosis). Immunol Rev 2020;297:26-38.

54. Sprooten J, De Wijngaert P, Vanmeerbeek I, et al. Necroptosis in Immuno-Oncology and Cancer Immunotherapy. Cells 2020;9:1823.

55. Sansone C, Bruno A, Piscitelli C, et al. Natural Compounds of Marine Origin as Inducers of Immunogenic Cell Death (ICD): Potential Role for Cancer Interception and Therapy. Cells 2021;10:231.

56. Pribluda A, Elyada E, Wiener Z, et al. A senescence-inflammatory switch from cancer-inhibitory to cancer-promoting mechanism. Cancer Cell 2013;24:242-56.

57. Cohen R, Rousseau B, Vidal J, et al. Immune Checkpoint Inhibition in Colorectal Cancer: Microsatellite Instability and Beyond. Target Oncol 2020;15:11-24.

58. Snyder AG, Hubbard NW, Messmer MN, et al. Intratumoral activation of the necroptotic pathway components RIPK1 and RIPK3 potentiates antitumor immunity. Sci Immunol 2019;4:eaaw2004.